Cone spacing and waveguide properties from cone directionality measurements

Susana Marcos and Stephen A. Burns

Schepens Eye Research Institute, 20 Staniford Street, Boston, Massachusetts 02114

Received August 17, 1998; revised manuscript received December 14, 1998; accepted December 23, 1998

Reflectometric techniques estimate the directionality of the retinal cones by measuring the distribution of light at the pupil plane of light reflected off the bleached retina. The waveguide-scattering model of Marcos *et al.* [J. Opt. Soc. Am. A **15**, 2012 (1998)] predicts that the shape of this intensity distribution is determined by both the waveguide properties of the cone photoreceptors and the topography of the cone mosaic (cone spacing). We have performed two types of cone directionality measurement. In the first type, cone directionality estimates are obtained by measuring the spatial distribution of light returning from the retina with a single-entry pupil position (single-entry measurements). In the second type, estimates are obtained by measuring the total amount of light guided back through the pupil as a function of entry pupil position (multiple-entry measurements). As predicted by the model, single-entry measurements provide narrower distributions than the multiple-entry measurements, since the former are affected by both waveguides and scattering and the latter are affected primarily by waveguides. Measurements at different retinal eccentricities and at two different wavelengths are consistent with the model. We show that the broader multiple-entry measurements are not accounted for by cone disarray. Results of multiple-entry measurements are closer to results from measurements of the psychophysical Stiles–Crawford effect (although still narrower), and the variation with retinal eccentricity and wavelength is similar. By combining single- and multiple-entry measurements, we can estimate cone spacing. The estimates at 0- and 2-deg retinal eccentricities are in good agreement with published anatomical data. © 1999 Optical Society of America [S0740-3232(99)03205-6]

OCIS codes: 0330.4300, 330.5310, 330.5370.

1. INTRODUCTION

It is widely accepted that the cone photoreceptors in the human retina exhibit directional sensitivity.[1] If the cones are pointing toward the center of the pupil, light entering through the center of the pupil (or, equivalently, entering the cones along their axis) is perceived as brighter than the same light coming from the edge of the pupil (i.e., at a larger angle). The Stiles–Crawford effect of the first kind (SCE), as this effect is known, is typically measured by using psychophysical techniques.[2,3] Since normal photoreceptor directionality requires a normal cone morphology and relation to the extracellular space, photoreceptor directionality has been of clinical interest.[4–8] Unfortunately, the long experimental sessions and the high degree of cooperation required for the psychophysical measures have restricted the availability of these measurements.

Recently developed reflectometric techniques allow a much more rapid estimation of cone directionality.[9–12] The common principle of these techniques is that, when the photopigment is bleached, part of the light entering the cone inner segments is guided along the outer segment and then scattered back toward the region of the pupil corresponding to the axis of the cones. The relative luminous efficiency (in psychophysical measurements) or the distribution of the directed or guided reflectance (in the reflectometric measurements) is typically fitted at the plane of the pupil by a Gaussian function $I_{\max}10^{-\rho[(x-x_0)^2+(y-y_0)^2]}$, where x_0 and y_0 represent the coordinates of the peak location for which either the luminous efficiency or the guided reflectance is highest (i.e., the location at the pupil plane where the cones are aimed) and rho (ρ) is a measure of directionality (the higher rho, the more narrowly tuned the function). It has been reported that reflectometric techniques provide the same estimate for the location at the pupil plane to which the photoreceptors are oriented, although directionality is, in general, higher (higher rho values) in reflectometric measurements than in psychophysical measurements.[9,13,14]

A. Predictions of the Waveguide-Scattering Model

We have proposed a more complete model[15] of the intensity distributions measured at the plane of the pupil obtained in the reflectometric technique of Burns *et al.*[11] In this technique the distribution at the pupil plane of light reflected off the retina is imaged on a CCD camera, and a small patch of the bleached retina is illuminated in Maxwellian view. In our model we propose that the light distribution at the pupil plane is affected by both the waveguide properties of the photoreceptors and the interference of light re-emitted from the cones. Our assumption is that since the photoreceptors have slightly different lengths, light emerges from each cone with a different phase and interferes at the plane of the pupil. For the dimensions of the eye and cone mosaic, the effect is similar to that produced at the far-field plane by light scattered from a rough surface.[16] The scattering alone produces a Gaussian distribution at the pupil plane, and the rho value (ρ_{scatt}) depends on the spatial distribution of the

cones[15]: $\rho_{scatt} = k(f\lambda)^{-2}s^2$, where f is the axial length of the eye, λ is the wavelength, k is a constant,[15] and s is the row-to-row cone spacing.

As a result, the overall intensity distribution at the plane of the pupil is the product of two Gaussian distributions[15]: the angular distribution of light emitted by the cones (ρ_{wg}) and the Gaussian distribution caused by scattering. The rho value for the final distribution is then the sum of the rho values from the two components: $\rho = \rho_{scatt} + \rho_{wg}$.

The waveguide-scattering model[15] predicts that techniques measuring the waveguide properties of the cones alone should produce lower rho values (ρ_{wg}) than the rho value in the reflectometric technique of Burns *et al.*[11] In addition, according to the model, if the waveguide properties can be measured independently, both ρ_{wg} and ρ_{scatt} can be determined, and the cone spacing of the retinal mosaic can be calculated. In the current paper, we present a technique to separate these components and show that the resulting cone spacing agrees with anatomical estimates in normal subjects, supporting our model. In addition, we show that different reflectometric techniques are differentially sensitive to ρ_{wg} and ρ_{scatt}. This differential sensitivity can explain some of the differences in measurements of cone directionality between laboratories.

B. Single- and Multiple-Entry Photoreceptor Directionality Measurements

In the technique of Burns *et al.*,[11] typically a single image is measured for the entry pupil position that produces the highest directional intensity. This distribution is used to determine rho. If the entry location is moved away from this optimal entry pupil, less light is coupled into the photoreceptors, and consequently the amount of guided light reflected back from the photoreceptors decreases. According to our model,[15] although the shape of the light distribution depends on both waveguides and scattering, the total amount of guided light at each entry pupil location depends only on the angular tuning of the cones. As a result, the total amount of light guided as a function of entry pupil position represents a measure of the waveguide properties of the cones and should be more similar to psychophysical estimates of cone directionality than to the estimates from the conventional reflectometric technique. We will refer to the measurements based on a single intensity distribution at the pupil as single-entry reflectometric measurements. The measurements based on the estimation of the total guided intensity as a function of entry pupil will be referred to as multiple-entry reflectometric measurements, since they are derived from multiple images.

In this paper we present single- and multiple-entry measurements of photoreceptor directionality for a group of subjects. As predicted by the model,[15] multiple-entry measurements (that depend on the waveguide properties alone) provide consistently lower estimates of rho (broader functions) than the single-entry measurements. In Section 4 we study the potential role of cone disarray[17–19] on the measurements, and we compare these results with previous measurements of the SCE in the same subjects.[14] We also present cone spacing estimates obtained by applying the model to directionality measurements. We finally reinterpret the results from other reflectometric measurements[9,10,12] by applying the waveguide scattering model.

2. METHODS

A. Apparatus

We used an imaging reflectometer to measure the spatial distribution of the guided light reflected off the retina (single-entry measurements), as well as to measure the total amount of guided light reflected off the retina as a function of entry pupil position (multiple-entry measurements). The apparatus has been described previously.[11,15,18] Briefly, a 1-deg area of the retina is illuminated in Maxwellian view by projecting a 0.18-μm laser spot at the pupil plane. Green or red illumination light is provided by two He–Ne lasers (543 and 632 nm, respectively). A diode-pumped laser (532 nm) provides a wide bleaching field [$\sim 6 \times 10^5$ trolands (td)]. The position of both the entrance pupil and the retinal fixation location is under computer control. Light returning from the retina through a 2-deg retinal field stop is collected at the plane of the pupil by means of a high-resolution, scientific-grade, cooled CCD camera (Princeton Instruments), located in a pupil conjugate plane. A separate channel allows infrared viewing of the pupil and is used for centration and alignment of the subject to the instrument throughout the session. Subjects' head positions are stabilized by means of a bite bar and forehead rests.

Single-entry reflectometric measurements are based only on the spatial distribution of light guided toward the pupil within a single image. However, the new multiple-entry measurements require accurate measurements of relative intensity for all images within a session. To ensure that fluctuations in either the light source or the detector did not cause artifacts, the tip of a fiber optic collecting part of the output of the laser source was placed at a plane conjugate to the pupil and imaged together with light coming from the retina. Fluctuations were not detected within any single session, so we present unnormalized data.

B. Subjects and Conditions

Single- and multiple-entry reflectometric measurements were collected on three normal subjects (SM, JH, and SB), ages 27, 38, and 48, one female and two males. JH had deuteranomalous color vision. Subjects were dilated with 0.5% Mydriacil after informed consent was obtained.

Two retinal locations (0 and 2 deg temporal) were tested in all subjects. Measurements were made typically using green light (543 nm); for subject JH data were also collected using red light (632 nm).

C. Experimental Procedure

Previous measurements[13,15,18] on each subject provided an estimate of the entry location that produced the highest directionality. This location was taken as the optimal entry pupil for each subject: $(0, -1)$ for subject SM, $(-1, 1)$ for subject JH, and $(0, -2)$ mm for subject SB. Positive coordinates stand for temporal and superior co-

ordinates at the pupil plane, and negative coordinates stand for nasal and inferior coordinates at the pupil plane.

Series of images were obtained while the entry pupil was moved in 0.5-mm steps along the horizontal and vertical axes. Five consecutive images were obtained at each entry pupil position, and 6 to 11 entry positions were tested per axis. For a given wavelength, the intensity of the illuminating beam was kept constant throughout the experiment. For each condition the entire series was repeated at least once on a different day.

D. Data Analysis

Figure 1 sketches the basic idea of both single- and multiple-entry measurements and shows how to extract cone directionality information from the two types of measurement. Figure 1(a) represents a series of images obtained with the imaging reflectometer as the illumination beam moves horizontally across the pupil.

For the single-entry estimates of cone directionality [see Fig. 1(b)], images at the optimal entry pupil are processed as described elsewhere.[11,18] First, the corneal reflexes corresponding to the first and fourth Purkinje images are eliminated. The intensity distribution at the pupil plane is fitted with the following equation: $B + I_{\max}10^{-\rho_s[(x-x_0)^2+(y-y_0)^2]}$, where B is a constant that accounts for light diffusely reflected, forming a constant background that fills the pupil, and the second term is a two-dimensional Gaussian function that represents the light directly guided from the photoreceptors; $I_{\max}$ is the intensity at the peak, and it is highest for images obtained when illuminating through the optimal entry pupil; and ρ_s is the directionality factor. For each session and each condition (retinal eccentricity and wavelength), we select the ρ_s corresponding to the best fit (the lowest rms between measurement and fit). Final ρ_s's are averages across sessions.

For the multiple-entry estimates of cone directionality [see Fig. 1(c)], we did not use the same fitting procedure, since the quality of the fit is poor when $I_{\max}$ is small. Instead, we obtained estimates of the total guided intensity by analyzing the images directly. As above, corneal reflexes are eliminated. We select a small region of the pupil far from the distribution of guided light. The average intensity over that region is taken as an estimate of the diffuse background. The background is then subtracted from the image. The remaining total intensity in the image is used as an estimate of the total guided intensity. The total guided intensity (average over five measurements) as a function of entry pupil position is fitted to a Gaussian: $tgI_{\max}10^{-\rho_{mx}(x-x_0)^2}$ and $tgI_{\max}10^{-\rho_{my}(y-y_0)^2}$ for the horizontal and vertical axes, respectively. If the spa-

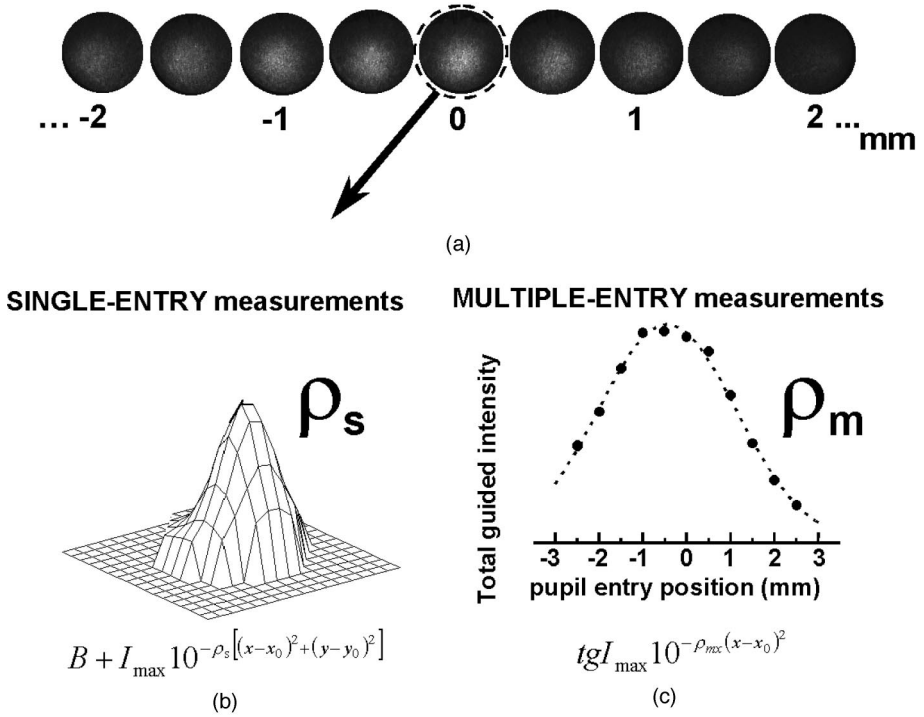

Fig. 1. Theory of single- and multiple-entry reflectometric measurements. The intensity distribution at the pupil plane of light returning from a small area of bleached retina is imaged on a CCD camera for a series of entry pupil locations [(a), data from subject SM, 0 deg, 543 nm, horizontal axis]. The total amount of guided light is maximum for the location in the pupil toward which the photoreceptors are pointing. The circled image corresponds to the optimal entry pupil location and is the image used for single-entry reflectometric measurements. Since these measurements are based on a single image, we refer to them as single-entry measurements [(b)]. The intensity distribution for the optimal image is fitted to a constant added to a two-dimensional Gaussian function, from which we obtain the rho value: ρ_s. As the entry position of the illuminating beam moves away from the optimal entry pupil, less light is captured by the cones and guided back. The measurements based on a series of images across the pupil are referred to as multiple-entry measurements [(c)]. The total amount of guided light as a function of entry pupil position is fitted with a Gaussian function, with the rho value ρ_{mx}. The final rho, ρ_m, is computed as the mean of the estimates for the horizontal and vertical axes (ρ_{mx} and ρ_{my}).

tial distribution of the guided light at the pupil plane fits a Gaussian whose rho value does not change with entry pupil position, then fitting the total guided intensity or the maximum of the guided intensity ($tgI_{\max}$) should be equivalent. We confirmed this by analyzing sample data both ways. We decided to use the total guided intensity instead of the maximum guided intensity because the first is based on the entire image and is therefore a more robust estimate.

For each session and each condition, ρ_m is obtained as the average of the rho values obtained by fitting the total guided intensity estimates across the horizontal and vertical axes [$\rho_m = (\rho_{mx} + \rho_{my})/2$]. Except for one case (SB, 0 deg), we did not find significant asymmetry between the estimates for the horizontal axis and the vertical axis. Final ρ_m's are averages across sessions. The peak locations (x_0 and y_0) obtained from the fit to the multiple-entry measurements [$(-0.15, -1.08)$ for SM, $(-1.09, 0.79)$ for JH, and $(-0.54, -2.24)$ mm for SB, on average] are similar to those obtained from single-entry measurements: $(-0.28, -1.29)$ for SM, $(-1.01, 0.77)$ for JH, and $(-0.07, -2.24)$ mm for SB, on average. These peak locations are very close to the horizontal and vertical coordinates chosen for the multiple-entry measurements. The reader should note that even if the sample transverse does not pass through the true peak location, the values of rho and the coordinates of the maximum would be constant, because of the nature of the Gaussian function that we are using in our analysis.[20]

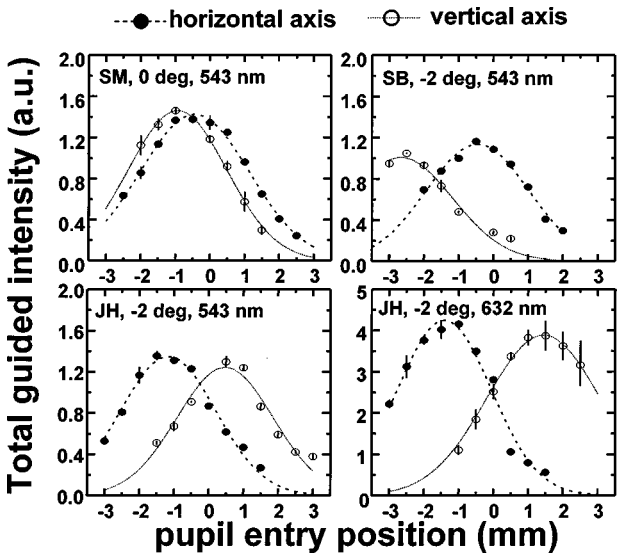

Fig. 2. Example of multiple-entry reflectometric functions (total guided intensity as a function of entry pupil position) for different subjects (SM, SB, and JH), retinal eccentricities (0 and 2 deg temporal), and wavelengths (543 and 632 nm). Each panel represents results from a single session. Circles are averaged across five consecutive measurements at the same pupil location. Filled circles stand for measurements across the horizontal axis, and open circles stand for measurements across the vertical axis. (Error bars stand for ±1 standard error of the mean.) Positive entry pupil positions stand for temporal and superior locations, and negative positions stand for nasal and inferior locations. Dashed and dotted curves represent the best fit to the measurements across the horizontal and vertical axes, respectively.

3. RESULTS

A. Single- and Multiple-Entry Directionality Measurements

Figure 1(a) shows a typical example of the intensity distribution at the pupil plane for a series of entry pupil positions (subject SM, 0 deg, horizontal axis). Single-entry rhos (ρ_s) are extracted from images obtained at the optimal entry pupil.

Figure 2 shows various representative examples of multiple-entry reflectometric functions for different subjects and conditions, obtained in separate sessions. Filled symbols represent measurements across the horizontal axis of the pupil, and open symbols represent measurements across the vertical axis. Each symbol is the average of five measurements, obtained consecutively. Reproducibility within a session is high (in most cases the error bars, ±1 standard error of the mean, are smaller than the size of the symbols). The measurements were well fitted by Gaussian functions (represented by dashed and dotted curves for the fits to measurements across the horizontal and vertical axes, respectively). Variability is highest for red illumination, probably because the background component is generally higher than the guided component, and slight errors in the determination of the background have a higher impact on the estimate of the total guided component than for green illumination.

B. Variation of Rho Value as a Function of Retinal Eccentricity and Wavelength

As our model predicts,[15] multiple-entry reflectometric functions are systematically broader (lower rho) than single-entry reflectometric distributions (higher rho). The difference is particularly clear at 2 deg, although at the center of the fovea, it is significant in two of the three subjects. Also, the increase of rho with retinal eccentricity is steeper for single-entry measurements than for multiple-entry measurements. Figure 3(a) shows rho derived from the two types of measurement as a function of retinal eccentricity for the three subjects, with the use of green (543-nm) light. Filled symbols represent single-entry measurements (ρ_s), and open symbols represent multiple-entry measurements (ρ_m). Each symbol is the average of estimates of rho values from at least two sessions. Table 1 shows ρ_s and ρ_m values for 0 and 2 deg for the three subjects, as well as the standard deviations of the measurements.

Single-entry measurements are markedly broader for red light than for green light, as shown elsewhere.[15] However, multiple-entry measurements are not significantly different for the two wavelengths. Figure 3(b) shows rho value as a function of retinal eccentricity for the two wavelengths for subject JH. Circles represent single-entry measurements, and squares represent multiple-entry measurements. Filled symbols stand for 543 nm, and open symbols stand for 632 nm. Whereas for single-entry measurements, rho (ρ_s) decreases as the wavelength increases, for multiple-entry measurements rho (ρ_m) is very similar for the two wavelengths.

4. DISCUSSION

Our model predicts that the spatial distribution of light guided back through the pupil is controlled by two factors:

waveguide properties and interference effects arising from the retinal cone mosaic.[15] We have separated these two factors by measuring cone directionality using two different approaches (measuring the spatial intensity distribution at the plane of the pupil for the optimal entry position and computing the total amount of light guided as a function of entry pupil position). As expected, multiple-entry measurements produce lower estimates of rho values than single-entry measurements, since the former should depend only on the waveguide properties, whereas the latter incorporate the additional contribution of scattering.

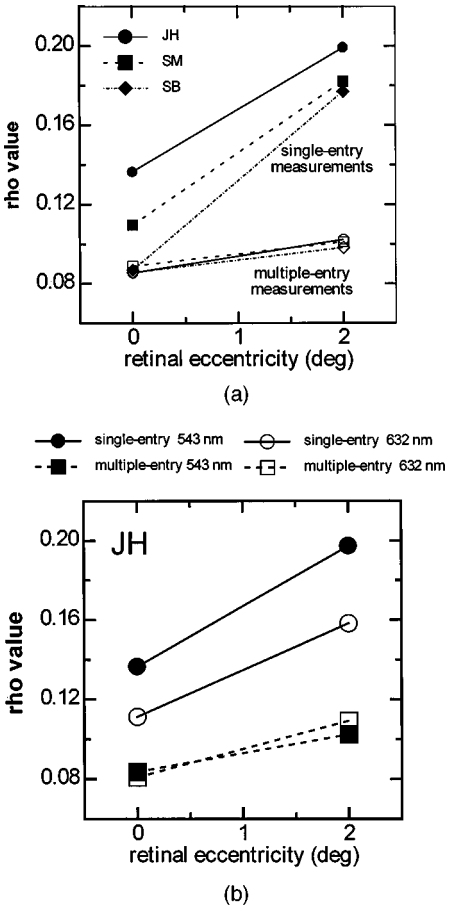

Fig. 3. Rho value as a function of retinal eccentricity for single-entry measurements ρ_s and multiple-entry measurements ρ_m. (a) Results for the three subjects. Symbols with the same shape correspond to the same subject. Single-entry measurements (filled symbols) are in all cases narrower than multiple-entry measurements (open symbols). (b) Results for subject JH for two wavelengths: 543 nm (filled symbols) and 632 nm (open symbols). Circles represent single-entry measurements, and squares represent multiple-entry measurements. Single-entry measurements are narrower in green light than in red light; however, there is no significant difference across wavelengths for multiple-entry measurements. Standard errors are smaller than 0.0166 mm^{-2} for single-entry measurements and smaller than 0.0108 mm^{-2} for multiple-entry measurements.

In Subsection 4.A we discuss the potential effects of photoreceptor disarray and show that they are not responsible for the differences that we find between the two measurements.

A. Effect of Cone-Photoreceptor Disarray

Photoreceptor disarray can potentially broaden the multiple-entry measurements with respect to single-entry measurements: if there are cones at an angle away from the group mean, those cones will return relatively more light at an angle of illumination along their own axis, corresponding to an entry pupil away from the optimal location. As a consequence, the multiple-entry measurements will broaden. Previous measurements show that cone disarray is small in the human fovea and parafovea.[17,18] MacLeod[17] calculated that the acceptance angle of an individual cone is only 2% less than the global tuning of a group of photoreceptors when a realistic amount of disarray is considered.

To calculate the possible influence of disarray on our measurements, we simulated the differences between single- and multiple-entry measurements in the presence of cone disarray (assuming the extreme case of no interference effects being involved). Figure 4 shows the rationale that we followed in the computer simulation. We assume that the cones have a given distribution of orientations[19] or distribution of pupil intercepts, using the same terminology as that used by MacLeod[17]: G_{dis}. In our calculations G_{dis} is a Gaussian function, but for simplicity in Fig. 4 we represent it as three delta functions. The emission angle of a single cone is also represented as a Gaussian function at the pupil plane, G_{wg}. For convenience, we suppose that both G_{dis} and G_{wg} are concentric with the geometrical center of the pupil: $10^{-\rho_{\mathrm{dis}}(x^2+y^2)}$ and $10^{-\rho_{\mathrm{wg}}(x^2+y^2)}$. We then compute the intensity distribution at the pupil plane for different entry pupils across the horizontal axis by performing the following convolution:

$$[G_{\mathrm{wg}}(x - x_i)G_{\mathrm{dis}}] * G_{\mathrm{wg}},$$

where x_i represents the entry pupil position of the illuminating beam. G_{dis} is multiplied by G_{wg}, since the amount of light captured by cones not oriented along the

Table 1. ρ_s and ρ_m for 0- and 2-deg Retinal Eccentricity (Three Subjects and Average) for the Experiments in the Present Study

	ρ_s (±1 standard deviation)		ρ_m (±1 standard deviation)	
Observer	0 deg	2 deg	0 deg	2 deg
JH	0.136 ± 0.004	0.197 ± 0.004	0.111 ± 0.012	0.102 ± 0.015
SM	0.110 ± 0.014	0.182 ± 0.023	0.089 ± 0.010	0.106 ± 0.017
SB	0.083 ± 0.002	0.189 ± 0.020	0.082 ± 0.015	0.093 ± 0.007
Average	0.110	0.189	0.094	0.100

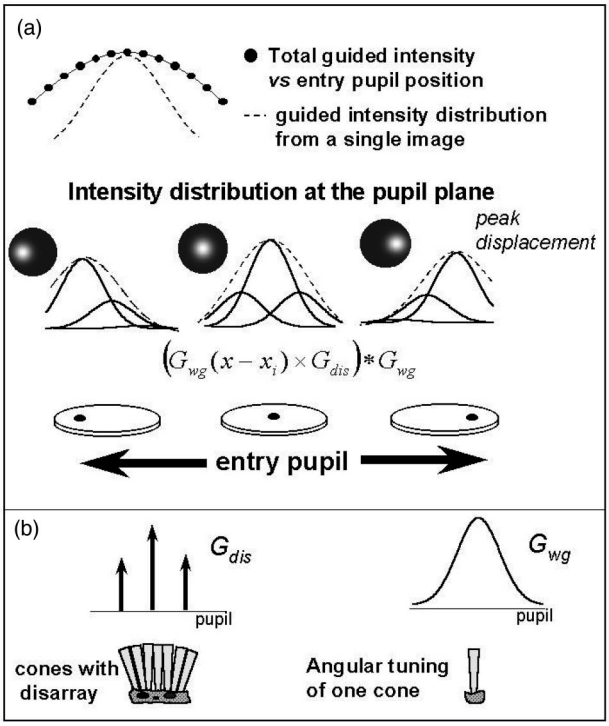

Fig. 4. Scheme of computer simulations showing the effect of cone disarray. G_{dis} stands for the cone disarray distribution (a Gaussian distribution in the simulation, represented as three delta functions for graphical purposes), and G_{wg} represents the angular tuning of a cone [(b)]. Part (a) represents the convolution process to compute the intensity distribution at the pupil plane for different entry pupil positions (shown for entry pupil positions coincident with the location of the delta functions). Cone disarray has two consequences: displacement of the peak of the intensity distribution and broadening of the function calculated as the total guided intensity versus pupil position with respect to the distribution computed from a single image.

direction of illumination is proportional to both the number of cones oriented toward a specific location at the pupil and the intensity of the tail of the angular tuning at that particular pupil location. Significant disarray predicts two findings[18] (Fig. 4): first, the location of the peak of the intensity distribution should move toward the direction of the entry pupil location; and second, the total guided intensity versus entry pupil position should be broader than the spatial intensity distribution from a single image. Both functions are affected by cone disarray, but single-entry measurements are affected to a lesser extent than multiple-entry measurements. From our simulations, and given values of G_{dis} and G_{wg}, we computed the displacement of the peak position and rho values for single- and multiple-entry measurements (ρ_s and ρ_m, respectively).

The actual measured variation in the location of the maximum in light exiting the eye was smaller than 0.5 mm when the entry location varied as much as 2.5 mm from the optimal entry pupil. We found similar peak displacements for both 0- and 2-deg retinal eccentricities and for both horizontal and vertical axes.

The simulations did not find a combination of waveguide properties and disarray that are consistent with both the peak displacements and broadening. We simulated single- and multiple-entry functions for different cases. For example, if we choose $\rho_{\mathrm{wg}} = 0.22\,\mathrm{mm}^{-2}$ and $\rho_{\mathrm{dis}} = 1.3\,\mathrm{mm}^{-2}$, we can compute single-entry intensity distributions ($\rho_s = 0.19\,\mathrm{mm}^{-2}$) to match our experimental estimates ($\rho_s = 0.189\,\mathrm{mm}^{-2}$, on average) at 2 deg; these conditions also generate peak displacements close to our experimental estimates (~0.5 mm). However, for these conditions the computed values for multiple-entry measurements ($\rho_m = 0.18\,\mathrm{mm}^{-2}$) do not match the experimental multiple-entry estimates ($\rho_m = 0.106\,\mathrm{mm}^{-2}$). In the example just shown, disarray would be responsible only for ~10% of the broadening that we found experimentally. If we choose $\rho_{\mathrm{wg}} = 0.12\,\mathrm{mm}^{-2}$ and $\rho_{\mathrm{dis}} = 0.8\,\mathrm{mm}^{-2}$, we can compute multiple-entry functions ($\rho_m = 0.10\,\mathrm{mm}^{-2}$) that match our experimental estimates for ρ_m and peak displacements. However, the predicted single-entry rho value ($\rho_s = 0.11\,\mathrm{mm}^{-2}$) is much lower than the experimental value. We conclude that another factor (scattering) must be involved in the differences between single- and multiple-entry measurements.

B. Reflectometric Measurements and the Stiles–Crawford Effect

Various studies show that estimates of the point in the pupil toward which the photoreceptors are optimally aligned agree well with measurements of the psychophysical SCE.[10,12,13,14] However, the directionality factor rho is consistently higher for reflectometric measurements than for psychophysical measurements. He *et al.*[14] compared in the same subjects the directionality factors obtained by using the reflectometric technique of Burns *et al.*[11] (single-entry measurements, using the terminology coined in the current paper) with psychophysical Stiles–Crawford measurements (using a criterion of flicker thresholds, and bleaching adaptation fields to avoid self-screening and to isolate as much as possible the waveguide properties). On average, rho for reflectometric measurements was ~2 × rho for the psychophysical measurements at the center of the fovea and ~4 × at −2-deg retinal eccentricity. Several causes are pointed to in that study to explain the narrowing of the single-entry reflectometric measurements.[14] Gorrand and Delori[21] proposed a model that explained the differences between psychophysical and reflectometric measurements, which suggested that some modes guided within the photoreceptors are poorly excited backward, giving rise to a narrowing of the reflected distribution. Although in some animals it is possible to image waveguides *in vivo*,[22] in humans it has not been possible; so although it is a plausible explanation, this hypothesis is not proven. Our model also predicted that single-entry reflectometric measurements should be broader than the psychophysical SCE measurements, since, according to the model, the former are affected by both waveguide properties and scattering, and the latter are affected primarily by the waveguide component.[15] According to our reasoning, multiple-entry measurements are also not affected by scattering from the cones and depend only on the waveguide properties of the photoreceptors. A question then

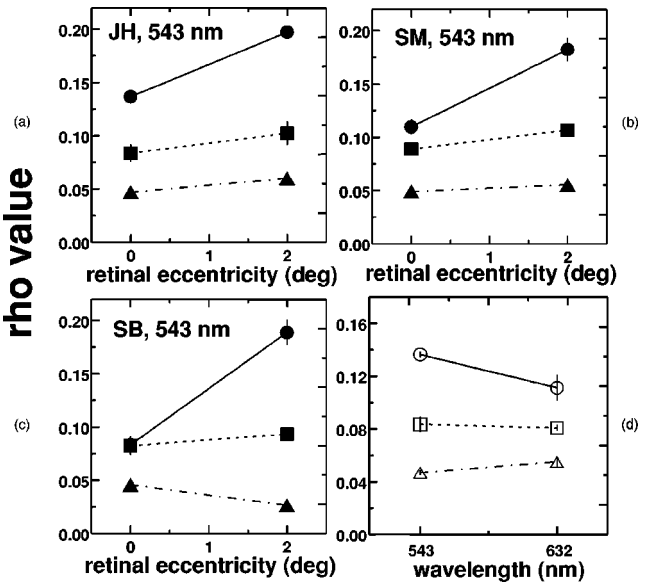

Fig. 5. Rho value as a function of retinal eccentricity for single-entry measurements ρ_s (filled circles), multiple-entry measurements ρ_m (filled squares), and Stiles–Crawford effect (SCE) measurements ρ_{SCE} from He *et al.*,[14] (filled triangles): (a) subject JH, (b) subject SM, and (c) subject SB. The variation of ρ_m and ρ_{SCE} with retinal eccentricity is similar; both increase more slowly with increasing retinal eccentricity than ρ_s. However, SCE measurements are still broader than multiple-entry measurements. (d) Rho value as a function of wavelength for subject JH: ρ_s (open circles), multiple-entry measurements ρ_m (open squares), and SCE measurements ρ_{SCE} (open triangles). ρ_s decreases markedly with wavelength, whereas ρ_{SCE} and ρ_m do not change significantly. Error bars represent ±1 standard error of the mean.

arises: do the SCE and multiple-entry reflectometric measurements reflect the same waveguide properties of the photoreceptors?

Results from the three types of measurement for the three subjects are displayed in Fig. 5. Figures 5(a), 5(b), and 5(c) show rho value as a function of retinal eccentricity for the single- and multiple-entry reflectometric measurements from the present study and SCE measurements from He *et al.*[14] for subjects JH, SM, and SB, respectively (who participated in both studies). ρ_{SCE} values are more similar to ρ_m values than to ρ_s values. The slight increase of SCE directionality with retinal eccentricity is consistent with previous data in the literature[23,24] and with predictions from waveguide models.[15,25] For all subjects both SCE and multiple-entry measurements vary with eccentricity more slowly than do the single-entry measurements. Figure 5(d) compares rho values as a function of wavelength for the three types of measurement for subject JH. Whereas single-entry measurements decrease markedly with wavelength, both SCE and multiple-entry measurements barely change. We had shown in a previous paper that the decrease of ρ_s with λ supports the presence of scattering[15,16]: the scattering component should decrease with wavelength, since it is inversely proportional to λ^2. In addition, our finding that both ρ_{SCE} and ρ_m change minimally with wavelength is consistent with the waveguide properties of the photoreceptors. Waveguide models predict a nonsystematic variation of rho as a function of wavelength, which is very dependent on the specific cone dimensions and indices of refraction.[25,26] In the bleached state,[27] the SCE measurements change little with wavelength.[28] Also, recent computer simulations of light propagation within the vertebrate retinal rod have shown a flat dependence of directionality with wavelength.[29]

Despite the parallel behavior of SCE and multiple-entry measurements as a function of retinal eccentricity and wavelength, we found that SCE functions are still broader than multiple-entry functions (ρ_{SCE} is shifted toward lower values). Such a discrepancy cannot be explained by our model. Chen and Makous[30] suggested cross talk (light escaping one cone and being absorbed in adjacent cones) as a potential reason for the broadening of the SCE with respect to the acceptance angle of a single cone. However, as has been pointed out,[14,30] cross talk is more likely at the foveal center, where the cones are more tightly packed, than at 2 deg, where the cone coverage is smaller. From Gorrand and Delori's model,[21] differences could also arise from differences between the angular dependence of the absorption and the emission of light by the photoreceptors. Finally, as demonstrated in Subsection 4.A, cone-photoreceptor disarray (which should contribute to a broadening of both SCE and multiple-entry measurements) seems a negligible factor.

C. Estimates of Cone Spacing

Our model predicts that $\rho_s = \rho_{wg} + \rho_{scatt}$, where ρ_{wg} is the angular tuning of the cone and ρ_{scatt} is given by scattering theory.[16] Since, assuming no disarray, $\rho_m = \rho_{wg}$, the scattering component can be derived by combining the two techniques: $\rho_{scatt} = \rho_s - \rho_m$. As we mentioned in Subsection 1.A, the scattering component (ρ_{scatt}) and the row-to-row cone spacing (s) are linked by the following expression:[15] $s = kf\lambda\sqrt{\rho_{scatt}}$, where $k = 1.20753$ (assuming cone apertures that are equal to 80% of the cone spacing), f is the axial length of the eye in

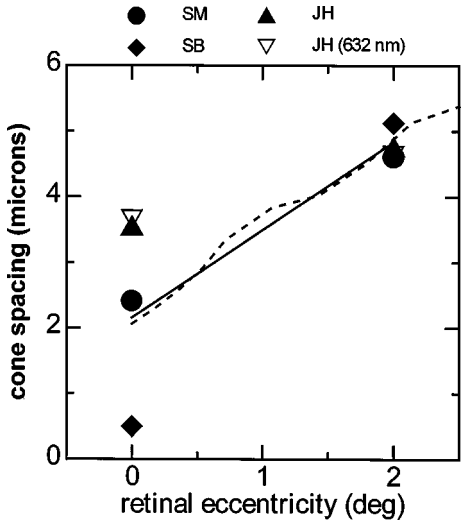

Fig. 6. Derived cone spacing as a function of retinal eccentricity for the three observers. Filled symbols are results using green light, and open symbols are results using red light. Solid line, average across the three subjects; dashed curve, average of anatomical data of Curcio *et al.*[31]

millimeters, and λ is the wavelength used in the experiments (0.543 and 0.632 μm). Figure 6 shows the calculated row-to-row cone spacing as a function of retinal eccentricity for the three subjects. The axial length of the eye was measured for each of the three subjects by using A-scan ultrasonography (f = 25.30 mm for SB, f = 25.52mm for SM, and f = 23.60 mm for JH). Filled symbols represent cone spacing estimates for the three subjects with green light. Open symbols are independent measurements using red light for JH. The solid line represents an average across our subjects, and the dashed curve is an average from the data of Curcio *et al.*,[31] which is very close to our average data. Note that, as in previous anatomical[31] and *in vivo*[32] cone spacing estimates, intersubject variability is higher at the foveal center than at 2-deg eccentricity.

In its present form, obtaining cone spacing is slower and more indirect than alternative imaging techniques.[32–34] However, the fact that we obtain consistent estimates of cone spacing provides further support for the waveguide-scattering model, suggesting that more information can be extracted from reflectometric directionality measurements than had been assumed.

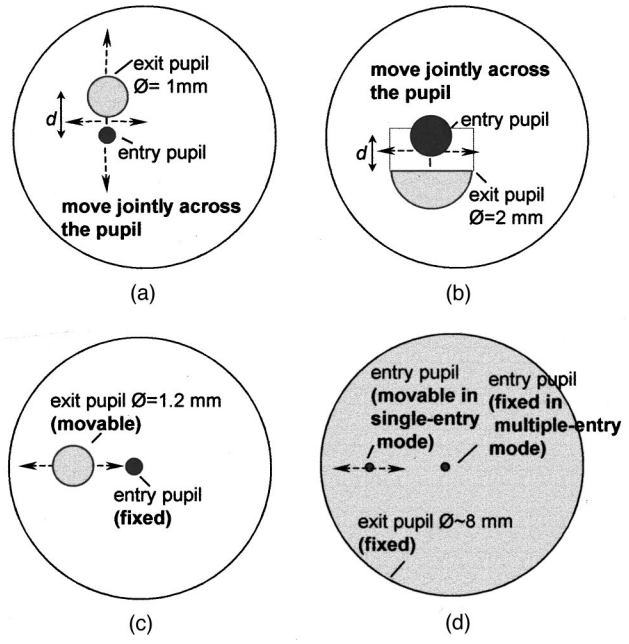

Fig. 7. Entry and exit pupil configurations in different cone directionality reflectometric techniques: (a) Gorrand and Delori,[10] (b) de Lint *et al.*,[12] (c) van Blokland,[9] (d) Burns *et al.*[13] and present paper.

D. Interpretation of Other Cone Directionality Techniques Using the Waveguide-Scattering Model

Although reflectometric techniques used to measure cone directionality are all based on the measurement of light reflected back from the cones with bleached photopigment, the particular design of each approach yields somewhat different rho directionality factors. By taking into account the particular optical configuration and experimental conditions, our model allows us to improve the comparability of the different techniques.

Figure 7 compares the pupil configurations for the techniques of Gorrand and Delori,[10] de Lint *et al.*,[12] and van Blokland[9] and the single- and multiple-entry techniques presented in the current paper. The sampled retinal area is 1 deg in our measurements as well as in those of Gorrand and Delori, 1.5 deg in those of van Blokland, and 2 deg in those of de Lint *et al.*[35] Wavelengths are also comparable: 543 nm in the study of Gorrand and Delori and in ours, 514 nm in that of de Lint *et al.*, and 568 nm in that of van Blokland.

Gorrand and Delori[10] scanned the exit and entry circular pupils across the eye's pupil. De Lint *et al.*[12] also used a double scanning configuration, with the exit pupil being a half-aperture of bigger radius than that of Gorrand and Delori (2 mm instead of 1 mm); however, they scanned only across the horizontal axis and measured the intensity distribution at a plane conjugate to the retina instead of in the pupil plane. These two techniques should yield similar rho values (as, in fact, they do in different sets of subjects). Apart from the difference in the exit pupil sizes and the distance between entry and exit pupils, the main difference must arise from the size of the sampled retina: that of de Lint *et al.* averaged over 2 deg, providing higher estimates of rho value.[35] Compared with our measurements, both approaches represent intermediate conditions between single- and multiple-entry measurements (ignoring the effects of instrumental anisotropy and design details such as the finite size of the sampling exit pupil aperture) the directionality is given by $\rho_s + \rho_m$ or $2\rho_{wg} + \rho_{\text{scatt}}$. That is, according to our model, these two techniques are affected twice by the waveguide properties (owing to the double scanning) as

Table 2. Values for Configurations of $\rho_{\text{Gorrand–Delori}}$, $\rho_{\text{de Lint } et\ al.}$, and $\rho_{\text{van Blokland}}$ (0 and 2 deg): Simulations Based on Results from Our Experiments and Experimental Values Reported in the Literature

	$\rho_{\text{Gorrand–Delori}}$		$\rho_{\text{de Lint } et\ al.}$		$\rho_{\text{van Blokland}}$	
Subject	0 deg	2 deg	0 deg	2 deg	0 deg	2 deg
Simulated						
JH	0.250	0.298	0.229	0.261	0.134	0.189
SM	0.202	0.288	0.187	0.256	0.198	0.176
SB	0.175	0.281	0.165	0.246	0.083	0.182
Average	0.209	0.289	0.194	0.254	0.108	0.182
Experimental[a]						
Average	0.204	0.279	0.226	Not reported	0.103	Not reported

[a] From the literature.[9,10,12]

well as by cone spacing. Increasing the exit pupil aperture should decrease rho—with the limiting case being a sampling aperture that fills the dilated pupil at all locations, as we have in our multiple-entry measurements. Van Blokland[9] scanned the exit pupil with a 1.2-mm pupil aperture while the illumination beam entered the eye through a fixed location. This configuration is equivalent to our single-entry measurements. In our case we image the pupil all at once, whereas van Blokland obtained sequential measurements along one axis.

Table 2 shows simulated rho values derived from the measurements on our subjects (with use of the rho values of Table 1) for other groups' configurations: those of Gorrand and Delori,[10] de Lint *et al.*,[12] and van Blokland[9] and the corresponding rho values reported from these groups.[9,10,12] We have used our fitted rhos and translated the maximum intensities to the center of the pupil. In addition, we simulated Gorrand and Delori's technique[10] only for a scan along the horizontal axis instead of scanning the entire pupil. The predictions from the simulations of the results from other techniques agree well with the experimental findings. As expected, the simulations of Gorrand and Delori's measurements[10] are slightly narrower than the simulations for the measurements of de Lint *et al.*[12] (unlike the experimental measurements). We believe that the reason[35] for the increase of the experimental rho value of de Lint *et al.* with respect to the simulated rho value is their increase in the sampled retinal area.[18] Both sets of data[10,12] are narrower than our single- and multiple-entry measurements as well as van Blokland's.[9]

5. CONCLUSIONS

From the single- and multiple-entry reflectometric measurements of cone directionality, we can conclude the following:

1. Single-entry reflectometric measurements (based on a single image) depend on waveguide properties and scattering from the photoreceptors.

2. Multiple-entry reflectometric measurements (based on a series of images with different pupil entry locations) depend primarily on the waveguide properties of the cones and thus are fitted by broader functions than the single-entry measurements.

3. The differences between single- and multiple-entry measurements cannot be accounted for by photoreceptor disarray.

4. The estimates of cone spacing obtained by applying the model to the two sets of measurements agree well with anatomical data.

5. Multiple-entry reflectometric measurements are more similar to Stiles–Crawford measurements than single-entry reflectometric measurements. They follow similar dependencies with retinal eccentricity and wavelength. However, the Stiles–Crawford functions are still broader than the multiple-entry functions.

6. The waveguide model can be used to explain differences between estimates of cone directionality obtained with different reflectometric techniques.

ACKNOWLEDGMENTS

We thank Ji Chang He for his help as an experimenter and as a subject and Dennis Donovan for performing the ultrasonography. This research was supported by National Institutes of Health grant EY-04395, DOE-DE-FG-02-91ER61229, and by the Massachusetts Lions Eye Research Foundation. S. Marcos was supported by Human Frontier Science Program Postdoctoral Fellowship LT542/97.

Address correspondence to Susana Marcos at the location on the title page or by phone, 617-912-2520, ext. 0520; fax, 617-912-0111; or e-mail, susana@vision.eri.harvard.edu.

REFERENCES AND NOTES

1. W. S. Stiles and B. H. Crawford, "The luminous efficiency of rays entering the eye pupil at different points," Proc. R. Soc. London, Ser. B **112**, 428–450 (1933).
2. J. M. Enoch and H. E. Bedell, "The Stiles–Crawford effects," in *Vertebrate Photoreceptor Optics*, J. M. Enoch and F. L. Tobey, eds., Springer Series in Optical Sciences (Springer, Heidelberg, 1981).
3. R. A. Applegate and V. Lakshminarayanan, "Parametric representation of Stiles–Crawford functions: normal variation of peak location and directionality," J. Opt. Soc. Am. A **10**, 1611–1623 (1993).
4. J. J. Vos and A. Huigen, "A clinical Stiles–Crawford apparatus," Am. J. Optom. Arch. Am. Acad. Optom. **39**, 68–76 (1962).
5. F. Fankhauser, J. M. Enoch, and P. Cibis, "Receptor orientation in retinal pathology," Am. J. Optom. Physiol. Opt. **55**, 807–812 (1978).
6. V. C. Smith, J. Pokorny, and K. R. Diddie, "Color matching and Stiles–Crawford effect in central serous detachment repair," Mod. Probl. Ophthalmol. **19**, 284–295 (1978).
7. J. Pokorny, V. C. Smith, and P. B. Johnston, "Photoreceptor misalignment accompanying a fibrous scar," Arch. Ophthalmol. (Chicago) **97**, 867–869 (1979).
8. C. R. Fitzgerald, D. G. Birch, and J. M. Enoch, "Functional analysis of vision in patients following retinal detachment repair," Arch. Ophthalmol. (Chicago) **98**, 1237–1244 (1980).
9. G. J. van Blokland, "Directionality and alignment of the foveal photoreceptors assessed with light scattered from the human fundus in vivo," Vision Res. **26**, 495–500 (1986).
10. J. M. Gorrand and F. C. Delori, "A reflectometric technique for assessing photoreceptor alignment," Vision Res. **35**, 999–1010 (1995).
11. S. A. Burns, S. Wu, F. C. Delori, and A. E. Elsner, "Direct measurement of human cone-photoreceptor alignment," J. Opt. Soc. Am. A **12**, 2329–2338 (1996).
12. P. J. de Lint, T. T. J. M. Berendschot, and D. van Norren, "Local photoreceptor alignment measured with a scanning laser ophthalmoscope," Vision Res. **37**, 243–248 (1997).
13. S. A. Burns, A. E. Elsner, J. M. Gorrand, M. R. Kreitz, and F. C. Delori, "Comparison of reflectometric and psychophysical measures of cone orientation," in *Noninvasive Assessment of the Visual System*, Vol. 1 of 1992 OSA Technical Digest Series (Optical Society of America, Washington, D.C., 1992), pp. 160–163.
14. J. C. He, S. Marcos, and S. A. Burns, "Comparison of cone directionality measured using psychophysical and reflectometric techniques," submitted to J. Opt. Soc. Am. A.
15. S. Marcos, S. A. Burns, and J. C. He, "A model for cone directionality reflectometric measurements based on scattering," J. Opt. Soc. Am. A **15**, 2012–2022 (1998).
16. P. Beckmann and A. Spizzino, *The Scattering of Electromagnetic Waves from Rough Surfaces* (Pergamon, New York, 1963).
17. D. I. A. MacLeod, "Directionally selective light adaptation:

a visual consequence of receptor disarray?" Vision Res. **14**, 369–378 (1974).
18. S. A. Burns, S. Wu, J. C. He, and A. E. Elsner, "Variations in photoreceptor directionality across the central retina," J. Opt. Soc. Am. A **14**, 2033–2040 (1997).
19. V. Lakshminarayanan and J. M. Enoch, "Shape of the Stiles–Crawford function for traverses of the entrance pupil not passing through the peak of sensitivity," Am. J. Optom. Physiol. Opt. **62**, 127–128 (1985).
20. A. Safir and L. J. Hyams, "Distribution of cone orientations as an explanation of the Stiles–Crawford effect," J. Opt. Soc. Am. **59**, 757–765 (1969).
21. J. M. Gorrand and F. C. Delori, "A model for assessment of cone directionality," J. Mod. Opt. **44**, 473–491 (1997).
22. G. Li, H. Zwick, R. Elliott, A. Akers, and B. E. Stuck, "Mode structure alterations in normal and laser exposed vertebrate photoreceptors in the small high numerical aperture of the snake," presented at the OSA Annual Meeting, Baltimore, Md., October 4-9, 1998.
23. G. Westheimer, "Dependence of the magnitude of the Stiles–Crawford effect on retinal location," J. Physiol. (London) **192**, 309–315 (1967).
24. J. M. Enoch and G. M. Hope, "Directional sensitivity of the foveal and parafoveal retina," Invest. Ophthalmol. Visual Sci. **12**, 497–503 (1973).
25. A. W. Snyder and C. L. Pask, "The Stiles–Crawford effect: explanation and consequences," Vision Res. **13**, 1115–1137 (1973).
26. J. M. Enoch, "Optical properties of the retinal receptors," J. Opt. Soc. Am. **53**, 71–85 (1963).
27. N. D. Miller, "The changes in the Stiles–Crawford effect with high luminance adapting fields," Am. J. Optom. Arch. Am. Acad. Optom. **41**, 599–608 (1964).
28. S. J. Starr, "Effect of luminance and wavelength on the Stiles–Crawford effect in dichromats," Ph.D. dissertation (University of Chicago, Chicago, Ill., 1977).
29. M. J. Piket-May, A. Taflove, and J. B. Troy, "Electrodynamics of visible light interactions with the vertebrate retinal rod," Opt. Lett. **18**, 568–570 (1993).
30. B. Chen and W. Makous, "Light capture by human cones," J. Physiol. (London) **190**, 583–593 (1989).
31. C. A. Curcio, K. R. Sloan, R. E. Kalina, and A. E. Hendrickson, "Human photoreceptor topography," J. Comp. Neurol. **292**, 497–523 (1992).
32. S. Marcos, R. Navarro, and P. Artal, "Coherent imaging of the cone mosaic in the living human eye," J. Opt. Soc. Am. A **13**, 897–905 (1996).
33. D. T. Miller, D. R. Williams, G. M. Morris, and J. Liang, "Images of the cone photoreceptors in the living human eye," Vision Res. **36**, 1067–1079 (1996).
34. A. R. Wade and F. W. Fitzke, "High-resolution imaging of the human cone photoreceptor mosaic using a laser scanning ophthalmoscope," Invest. Ophthalmol. Visual Sci. **39**, 204 (1998).
35. In de Lint *et al.*,[12] the sampled retinal area is in fact given by the angular pixel size in the scanning laser ophthalmoscope images. However, their processing includes pixel smoothing (10×10), and final rho values are given after subsequent spatial average across the 2-deg central region.